Frequency versus relaxation oscillations in a semiconductor laser with coherent filtered optical feedback

H. Erzgräber[1], B. Krauskopf[2,1], D. Lenstra[1,3], A.P.A. Fischer[4], and G. Vemuri[5]
[1] *Afdeling Natuurkunde en Sterrenkunde, Vrije Universiteit Amsterdam, De Boelelaan 1081, 1081 HV Amsterdam, The Netherlands*
[2] *Department of Engineering Mathematics, University of Bristol, Bristol BS8 1TR, UK*
[3] *Research Institute COBRA, Technical University Eindhoven, The Netherlands*
[4] *Laboratoire de Physique des Lasers, Université Paris XIII, UMR CNRS 7538, France*
[5] *Indiana University–Purdue University Indianapolis, IN 46202-3273, USA*
(Dated: November 16, 2005)

We investigate the dynamics of a semiconductor laser subject to coherent, delayed filtered optical feedback. This system produces multi-stable continuous wave, relaxation and pure frequency oscillations. We show that the feedback phase is a key quantity for controlling this dynamical complexity. A systematic analysis with the feedback phase as one bifurcation parameter reveals the system's overall dynamical structure.

PACS numbers: 42.65.Sf, 05.45.Xt, 02.30.Ks, 42.55.Px

In a system with feedback a part of the output re-enters into the system, possibly after having been manipulated externally. Typically, the feedback mechanism involves a time delay, which is substantial in many applications; see, *e.g.*, the recent studies Refs. [1–4]. Laser systems with delayed feedback are of particular interest, because of their possible practical applications, for example, for secure communication via a chaotic carrier [5–7].

In this paper we consider a semiconductor laser (SL) with filtered optical feedback (FOF), where the output light re-enters the SL after passing through a filter of a given central frequency and width. FOF has received quite some attention recently, because of the additional control over the behavior of the SL by the possibility of choosing the filter width and by changing the detuning between the laser and the filter [8, 9]. This can be used to obtain stable single-mode operation or to select a specific frequency of the system [10].

Filtered optical feedback as considered here is an example of coherent feedback, where both the amplitude and phase of the feedback are important. In coherent optical feedback the feedback signal accumulates a phase shift $C_p = \Omega_0 \tau$, where Ω_0 is the laser frequency and τ is the delay time. The feedback phase C_p controls the position of the solitary laser frequency Ω_0 with respect to the optical frequency comb of the external delay system, which is quite similar to the carrier off-set frequency in laser-based precision spectroscopy and optical frequency comb techniques [11]. This is in contrast to optical systems with incoherent feedback [10, 12–14] since these systems lack an underlying external frequency comb. For the case of conventional optical feedback it turns out that for sufficiently long delay times the external cavity mode spacing $\nu_{EC} \sim 1/\tau$ becomes very small and the number of modes increases so much that C_p has no influence anymore. On the other hand, for short delay times (on the order of or less than the characteristic relaxation oscillation period) the feedback phase becomes a key parameter [15–17]. We demonstrate here that the feedback phase C_p is important for the dynamics of the FOF laser even for relatively long delay times (larger than the relaxation oscillation period). In particular, C_p distinguishes between the large number of coexisting stable solutions.

The FOF laser has been studied by numerical integration of the governing rate equations (introduced below), which showed the existence of periodic, quasiperiodic and chaotic output, as well as good agreement between the rate equations and experiments [9, 18, 19]. How the continuous wave (CW) solutions — known as the external filtered modes (EFMs) — depend on the parameters is analyzed in Ref. [20]. Note that the EFMs are conceptually the same CW solutions as the external cavity modes of the conventional optical feedback laser [20].

We report here on qualitatively different types of oscillations of the FOF laser, which bifurcate when the EFMs lose their stability. In particular, we consider frequency oscillations (FOs), which were recently reported in Ref. [9], and we show that they occur stably in large regions of the parameter space. FOs are external roundtrip oscillations for which the optical frequency oscillates without measurable oscillations in the intensity. This is remarkable because the phase-amplitude coupling in SLs, described by the self-phase modulation parameter α, effectively leads to an intimate connection between intensity and phase oscillations.

The other type of oscillations studied here are the much better known relaxation oscillations (ROs), which are a periodic exchange of energy between the electric field and the inversion (number of electron-hole pairs) inside the laser at a frequency primarily determined by solitary laser parameters and only little influenced by the delay; see, *e.g.*, Refs. [21, 22].

In the coherent FOF setup, shown in Fig. 1, a part of the light emitted by the SL is spectrally filtered by a Fabry-Pérot interferometer and then re-injected into the SL after a fixed delay time. More specifically, at BS 1 50% of the light emitted by the laser enters the feedback loop, where optical isolators allow clockwise propagation

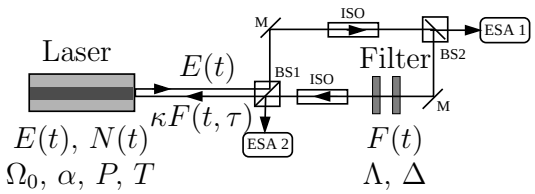

FIG. 1: Sketch of the experimental setup with the SL and the feedback loop with a Fabry-Pérot, beamsplitters (BS), optical isolator (ISO), mirrors (M) and electrical spectrum analyzer for measuring the dynamics of the SL (ESA 1) and feedback light (ESA 2).

only. The Fabry-Pérot with a finesse of ~ 5 is made of two parallel mirrors resulting in a transmission line shape that is approximated by a single Lorentzian. A pigtailed photodiode, an amplifier with a bandwidth of 500 MHz and an electrical spectrum analyzer (ESA) are used to measure the dynamical behavior of both the intensity emitted by SL and the intensity fed back into it. Great care has been taken to prevent unwanted feedback from the detection branches. Details about the experimental setup can be found in Ref. [18].

The FOF laser can be modeled by the rate equations

$$\dot{E} = (1+i\alpha)N(t)E(t) + \kappa F(t,\tau) \quad (1)$$

$$T\dot{N} = P - N(t) - (1+2N(t))|E(t)|^2 \quad (2)$$

$$\dot{F} = \Lambda E(t-\tau)e^{-iC_p} + (i\Delta - \Lambda)F(t)\,, \quad (3)$$

where time is measured in units of the photon lifetime (for SLs in the order of 10 ps), E and F are the complex envelopes of the optical field of the laser and filtered feedback field, respectively, and N is the inversion of the laser. The parameters are the self-phase modulation α, the feedback rate κ, the carrier life time T, the half width at half maximum (HWHM) of the filter Λ, the feedback phase C_p, the delay time τ, and the detuning Δ between the laser and the filter; see Ref. [20] for details of the model. These rescaled parameter values are chosen to represent the experimental conditions: $\alpha = 5.0$, $\tau = 500$, $\Lambda = 0.007$, $\Delta = -0.007$, $T = 100$ and $P = 3.5$.

We compute EFMs, ROs and FOs of the delay differential equation system (1)–(3) and determine their stability in dependence on the feedback rate κ and the feedback phase C_p. For this purpose we use the continuation software DDE-BIFTOOL [23].

Figure 2 depicts time series of Eqs. (1)–(3), namely, pure relaxation oscillations (a), pure frequency oscillations (b), and quasi-periodic frequency oscillations (c). Shown are the intensities $I_{L,F}$ and the frequencies $\dot{\Phi}_{L,F}$ of the laser field and the feedback field, respectively, where $E(t) = \sqrt{I_L(t)}e^{i\Phi_L(t)}$ and $F(t) = \sqrt{I_F(t)}e^{i\Phi_F(t)}$.

Figure 2(a) shows a typical example of ROs with a frequency of 4.2 GHz. (In an optical spectrum such ROs can be seen as side peaks.) Notice that, since the HWHM of the filter is narrow compared to the relaxation oscillation

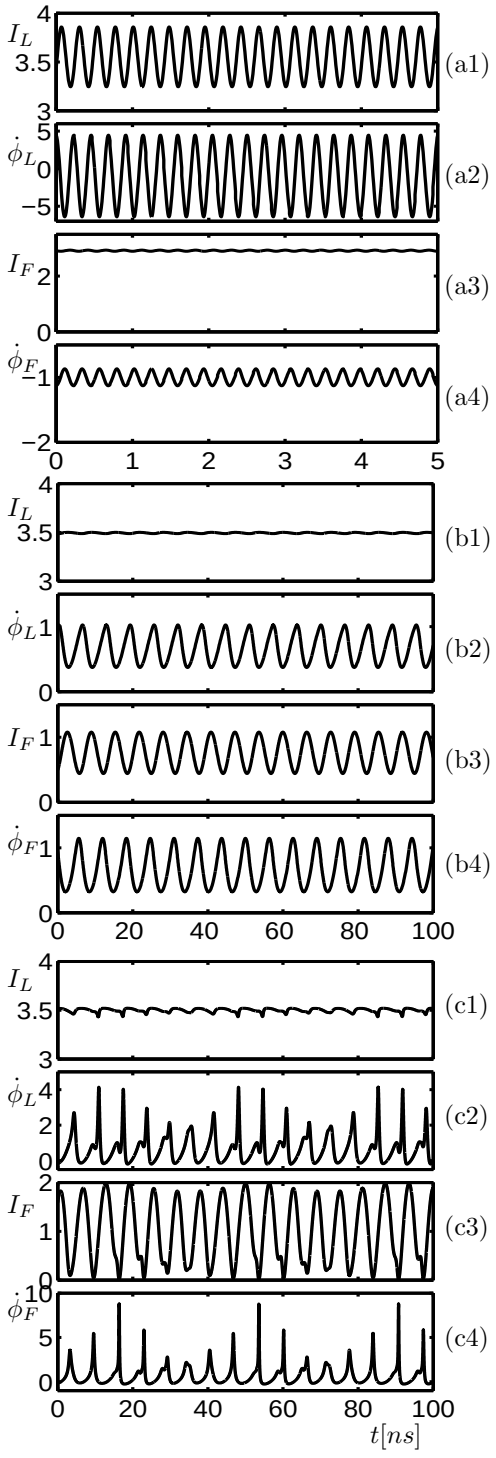

FIG. 2: Typical time series of I_L, I_F $\dot{\Phi}_L$ and $\dot{\Phi}_F$ of pure relaxation oscillations (a), pure frequency oscillations (b), and quasi-periodic frequency oscillations (c). Note the different time scales. From (a) to (c) (κ, C_p) takes the values $(0.02, -8/3\pi)$, $(0.07, -6\pi)$ and $(0.014, -6\pi)$.

frequency, the intensity I_F transmitted through the filter (and then fed back into the laser) is almost constant.

Thus, the filter efficiently blocks the fast relaxation dynamics and lets only the CW-component through. Effectively, the laser experiences constant weak optical injection that undamps ROs, which are much faster than the filter width. In Refs. [20, 24] it is discussed how FOF reduces to a laser with optical injection in the limit of a narrow filter. Physically, a narrow filter also means that the feedback light spends a long time $\sim \frac{1}{\Lambda}$ in the filter and makes the effective delay time very long.

That the dynamics of the filter has to be taken into account for an intermediate filter width as discussed here is evidenced by the presence of FOs, of which Fig. 2(b) shows an example. In contrast to the ROs discussed above, the intensity of the laser is almost constant, but its frequency $\dot{\Phi}_L$ oscillates with a period related to the roundtrip time in the feedback loop. (The period is actually longer because the filter adds a substantial frequency shift of $\sim \frac{1}{\Lambda}$.) The roundtrip time $\tau = 5$ ns corresponds to a frequency of 200 MHz, which is well within the filter width. Thus, both $I_F(t)$ and $\dot{\Phi}_F(t)$, and therefore the instantaneous feedback rate and phase, are oscillating. Note that the SL frequency $\dot{\Phi}_L(t)$ and the feedback intensity $I_F(t)$ are approximately in anti-phase for this FO. In Ref. [9] the FOs are interpreted as an interplay between the filter and the laser that compensates for the effects of the amplitude-phase coupling, leading to an effectively zero α-parameter. Also, in Ref. [8] it is argued that FOF, in this case from a double mirror, effectively reduces the value of α. Figure 2(b) allows us to characterize this interplay in more detail. Because of the filter the intensity of the feedback light changes according to the changes in the frequency of the laser. This results in a virtually constant intensity of the laser.

Finally, Fig. 2(c) shows that FOs can undergo further bifurcations, *e.g.*, leading to quasiperiodic dynamics after a torus bifurcation. This dynamical regime differs from the quasiperiodic dynamics associated with ROs, in that there is again only very small intensity dynamics. Notice that the FOs exhibits a slow modulation with a period about six time larger than the basic oscillation. This ratio may crucially depend on other parameters.

The regions of stability in the (κ, C_p)-plane of the EFMs, ROs, and FOs are shown in Fig. 3. They have been found by extensive numerical continuation of EFMs and the bifurcating periodic solutions. There is one large region of stable EFMs (light gray) and three large regions of stable oscillations (dark gray), namely one region of ROs and two separate regions of FOs. The FO shown in Fig. 2(b) is from the lower region. It features an approximate anti-phase relationship between $\dot{\Phi}_L(t)$ and $I_F(t)$, which is due to the fact that the dynamics take place on the right flank of the filter profile. In the upper region of FOs, on the other hand, the dynamics take place on the left flank of the filter profile and $\dot{\Phi}_L(t)$ and $I_F(t)$ are apprximately in phase. The boundaries between the different stability regions in Fig. 3 are bifurcation curves, where the dynamics changes qualitatively. Typically, EFMs are created in pairs (a stable and an unstable one) in saddle-node bifurcations (SN) and lose their stability in Hopf bifurcations (H). Depending on the values of κ and C_p, either ROs or FOs are born in this loss of stability of the EFMs. In turn, ROs and FOs can bifurcate in saddle-node bifurcations of limit cycles (SL) or lose their stability in a torus bifurcation (T), which leads to quasiperiodic oscillation. An example of quasiperiodic dynamics bifurcating from a FO is shown in Fig. 2(c). At a torus bifurcation the initial oscillation does not disappear, but can be followed as an unstable periodic orbit to detect further bifurcations. In particular, period-doubling of already unstable oscillations are found. In Fig. 3 we only show the boundaries of the regions of stability of EFMs, ROs, and FO; a more detailed discussion of the bifurcation diagram will be given elsewhere.

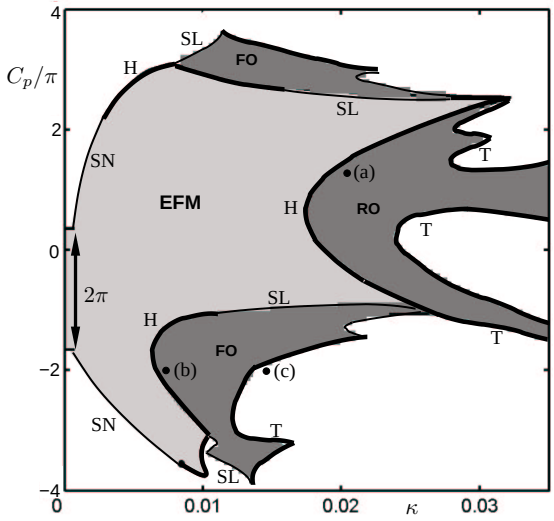

FIG. 3: Regions of different dynamics in the (κ, C_p)-plane. Light gray indicates stable EFMs and dark gray stable FOs or ROs. Thin lines indicate saddle-node (SN) or saddle-node of limit cycle (SL) bifurcations, and thick lines Hopf (H) or torus (T) bifurcations. The points with labels (a)–(c) indicate where the time series of Fig. 2 can be found.

The different stability regions in Fig. 3 extend over several periods of the 2π-periodic feedback phase C_p; the solution that can be followed from the solitary laser state is found for C_p around $-\pi$. Due to the periodicity of C_p, all 2π-shifted copies of these stability regions coexist, which leads to a large amount of multistability. In particular, it is possible that EFMs, ROs, and the two kinds of FOs coexist stably. Notice that, regardless of this multistability, the stability regions of FOs are accessible in an experiment by increasing the feedback rate κ from zero for a suitable choice of C_p.

Figure 4 shows characteristic experimental RIN-spectra of stable FOs, where the length of the feedback loop was measured to be $L = 1.55 \pm 0.01$ m, corresponding to a delay time $\tau = 5.17 \pm 0.04$ ns or a roundtrip frequency of $f_{ext} = 193 \pm 1$ MHz. The filter HWHM was

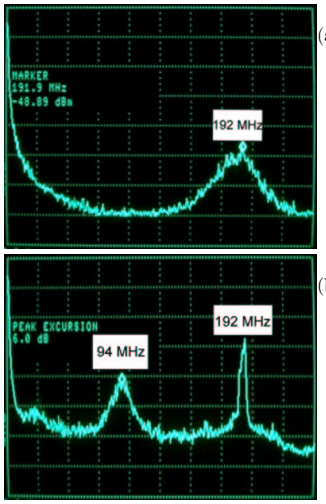

FIG. 4: Experimentally observed RIN-spectra of FOs, showing the intensity emitted by the SL (a), and the frequency of the SL, which is measured as the intensity that is fed back (b). Both spectra are in dB and cover the frequency range from 0 to 250 MHz.

900 MHz. Figure 4(a) shows the RIN of the intensity emitted by the SL (ESA 1) and Fig. 4(b) shows the RIN of the intensity fed back into the laser (ESA 1). In both spectra a peak T1 at 192 MHz can be seen, which corresponds to the roundtrip frequency f_{ext} within the experimental accuracy. The linewidth of the peak in Fig. 4(a) is very broad (about 20 MHz). Therefore, we interpret it as noise-enhanced dynamics of an unstable resonance condition in the feedback loop. The peak in Fig. 4(b), on the other hand, is very narrow and about 20 dB higher. This is a clear oscillation of optical frequency of the SL, converted into intensity by the operation of the filter and detected by the photodiode. Together these RIN-spectra constitute the characteristics of the theoretical FO dynamics in Fig. 3(b). The RIN in Fig. 4(b) also shows a smaller broad peak T2 at 94 MHz. Since T1 and T2 are in a ratio of 1:2 within the experimental accuracy, this might suggest a (noise-enhanced) precursor of a period-doubling bifurcation.

We showed that a semiconductor laser with filtered optical feedback supports fundamentally different oscillations, namely two kinds of pure frequency oscillations and characteristic relaxation oscillations. Both occur stably in large domains under variation of the feedback conditions. The feedback phase was recognized as the main distinguishing parameter. Our analysis characterizes the FOs in terms of the interplay between the SL field and the dynamics of the filter. Furthemore, we found two separate regions of FOs that differ in that the laser field intensity and the filtered field intensity are in-phase and anti-phase, respectively. The detailed analysis of FOs and their bifurcations is an interesting topic of ongoing investigations. Another interesting question is what kinds of more complicated dynamics, including quasi-periodicity and chaos, are possible when these oscillations become unstable.

G.V. was supported by the NSF and B.K. by an EPSRC Advanced Research Fellowship grant.

[1] C. Loewenich, H. Benner, and W. Just, Phys. Rev. Lett. **93**, 174101 (2004).
[2] A. Ahlborn and U. Parlitz, Phys. Rev. Lett. **63**, 264101 (2004).
[3] A. Roxin, N. Brunel, and D. Hansel, Phys. Rev. Lett. **94**, 238103 (2005).
[4] T. Piwonski, J. Houlihan, T. Busch, and G. Huyet, Phys. Rev. Lett. **95**, 040601 (2005).
[5] G. VanWiggeren and R. Roy, Science **279**, 1198 (1998).
[6] I. Fischer, Y. Liu, and P. Davis, Phys. Rev. A **62**, 011801(R) (2002).
[7] J.-P. Goedgebuer, L. Larger, and H. Porte, Phys. Rev. Lett. **80**, 2249 (1998).
[8] F. Rogister, P. Mégret, O. Deparis, M. Blondel, and T. Erneux, Opt. Lett. **24**, 1218 (1999).
[9] A. Fischer, M. Yousefi, D. Lenstra, M. Carter, and G. Vemuri, Phys. Rev. Lett. **92**, 023901 (2004).
[10] H. Yasaka and H. Kawagushi, Appl. Phys. Lett. **53(15)**, 1360 (1988).
[11] T. Udem, R. Holzwarth, and T. Hänsch, Nature **416**, 233 (2002).
[12] T. Heil, A. Uchida, P. Davis, and T. Aida, Phys. Rev. A **68**, 033811 (2003).
[13] B. Farias, T. P. de Silans, M. Chevrollier, and M. Oriá, Phys. Rev. Lett. **94**, 173902 (2005).
[14] L. Larger, P.-A. Lacourt, S. Poinsot, and M. Hanna, Phys. Rev. Lett. **95**, 043903 (2005).
[15] T. Heil, I. Fischer, W. Elsäßer, and A. Gavrielides, Phys. Rev. Lett. **87**, 243901 (2001).
[16] O. Ushakov, S. Bauer, O. Brox, H.-J. Wünsche, and F. Henneberger, Phys. Rev. Lett. **92**, 043902 (2004).
[17] A. Tabaka, K. Panajotov, I. Veretennicoff, and M. Sciamanna, Phys. Rev. E **70**, 036211 (2004).
[18] A. Fischer, O. Andersen, M. Yousefi, S. Stolte, and D. Lenstra, IEEE J. Quantum Electron. **36**, 375 (2000).
[19] M. Yousefi, D. Lenstra, and G. Vemuri, Phys. Rev. E **67**, 046213 (2003).
[20] K. Green and B. Krauskopf, Opt. Commun. **to appear** (2005).
[21] A. Tager and K. Petermann, IEEE J. Quantum Electron. **30**, 1553 (1994).
[22] B. Haegeman, K. Engelborghs, D. Rose, D. Pieroux, and T. Erneux, Phys. Rev. E **66**, 046216 (2002).
[23] K. Engelborghs, T. Luzyanina, and G. Samaey, *DDE-BIFTOOL v. 2.00 user manual: a Matlab package for bifurcation analysis of delay differential equations. Technical report TW-330* (Department of Computer Science, K.U. Leuven, Leuven, Belgium, 2001).
[24] T. Erneux, M. Yousefi, and D. Lenstra (2003), EQEC 2003, Munich, Europhysics Abstracts 27E, EA 04 THU.